LBNL 0000

Lawrence Berkeley National Laboratory

Extremum Seeking Control of Smart Inverters for VAR Compensation

Daniel Arnold [1], Matias Negrete-Pincetic [1], Emma Stewart [2], David M. Auslander [1], Duncan Callaway [1]

[1] U C Berkeley, Berkeley, CA

[2] Lawrence Berkeley National Laboratory, Berkeley, CA

September 2015

Power & Energy Society General Meeting, 2015 IEEE

This work has been funded partly by the Office of Electricity Delivery and Energy Reliability, Distributed Energy Program of the U.S. Department of Energy under Contract No. DE-AC02-05CH11231

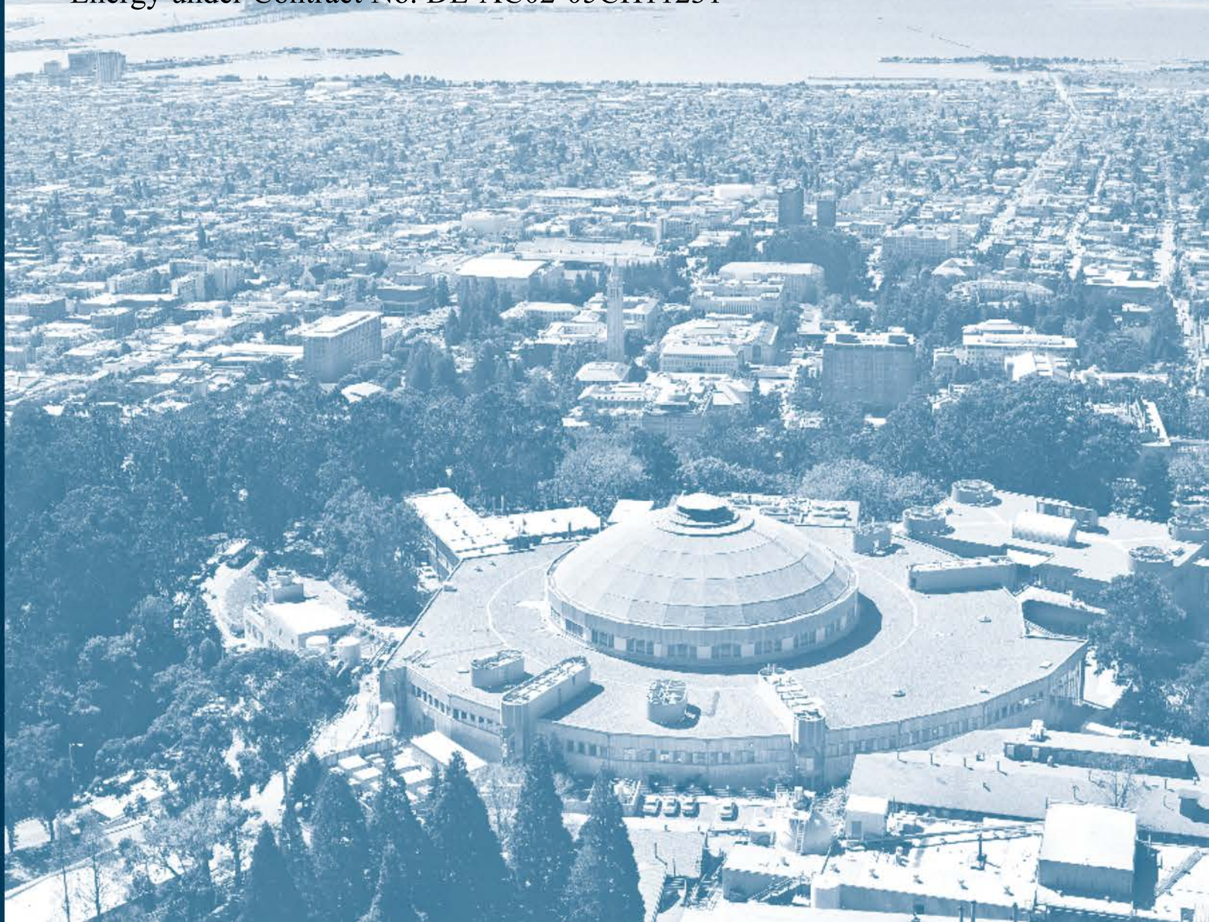

Extremum Seeking Control of Smart Inverters for VAR Compensation

Daniel B. Arnold, Matias Negrete-Pincetic, Emma M. Stewart, David M. Auslander, and Duncan S. Callaway

Abstract— **Reactive power compensation is used by utilities to ensure customer voltages are within pre-defined tolerances and reduce system resistive losses. While much attention has been paid to model-based control algorithms for reactive power support and Volt Var Optimization (VVO), these strategies typically require relatively large communications capabilities and accurate models. In this work, a non-model-based control strategy for smart inverters is considered for VAR compensation. An Extremum Seeking control algorithm is applied to modulate the reactive power output of inverters based on real power information from the feeder substation, without an explicit feeder model. Simulation results using utility demand information confirm the ability of the control algorithm to inject VARs to minimize feeder head real power consumption. In addition, we show that the algorithm is capable of improving feeder voltage profiles and reducing reactive power supplied by the distribution substation.**

I. Introduction

There are significant barriers that must be overcome to enable the deployment of high levels of renewables in the distribution system. Challenges primarily lie in managing an aging infrastructure and increasing reliability in the context of variable resources. As more distributed energy resources are incorporated into the system, feeder voltage profiles and reactive power flows must be carefully managed to ensure power of sufficient quality and quantity is available to retail customers at least cost. As has been experienced in Hawaii [1], the negative impact of high levels of distributed PV under current interconnection standards is significant, and has led to financial impacts to both consumers and the utility. Distributed resources could, under the correct operational control scenarios, provide numerous benefits to the grid, including voltage support and VAR compensation. At the moment, the restrictions imposed by IEEE 1547 prevent inverters from providing such utility to the system. However, ongoing efforts to refine this standard, along with California Rule 21, aim to allow more advanced control options for distributed inverters.

In the context of Volt-VAR Optimization (VVO), four quadrant inverters can be used to consume or supply reactive power [2] to improve feeder voltages. This is accomplished via either: 1) using excess inverter capacity not utilized for real power generation, or 2) a reduction in real power output to allow reactive power generation. While currently no incentive exists to support the latter activity, the potential systemic benefits are substantial [3].

Many of the inverter-based VVO strategies currently under investigation involve solving centrally-based optimization problems. The authors of [4] considered voltage regulation and loss minimization in distribution circuits using second order cone relaxations of balanced feeder models. The work in [5] and [6] have considered voltage regulation in distribution networks in the context of power flow through framing the decision process as a semidefinite program. The results of [5] provide conditions under which the semidefinite relaxation of the nonconvex power flow problem is tight in balanced distribution circuits. In [6], semidefinite relaxations are applied to unbalanced distribution systems, but no optimality conditions are provided. As these frameworks either depend on solving a centralized optimization or rely on information exchange between decision-makers, it would be necessary to develop an infrastructure to collect sensing information (such as real and reactive power demands) and relay data and actuation signals. This would come at a cost and could require the transfer of information across privately owned assets. Furthermore, for broad utilization it could require coordinating inverters from different manufacturers. In addition, many of these strategies require perfect knowledge of feeder characteristics, such as line segment impedances and network configuration. This information may not be readily available to utility operators.

In contrast, other inverter-based VVO strategies sacrifice optimality in favor of less reliance on required communications (i.e. decentralized approaches). The authors of [2] considered a suite of distributed control strategies for reactive power compensation using four quadrant inverters. The authors concluded that using local information alone is sufficient for voltage regulation, but the incorporation of real and reactive power flows improves control system performance. Using a fully decentralized approach, the work of [3] studied the effect of the shape of different inverter volt-var control curves for voltage regulation in high PV penetration scenarios.

In this work, we propose a method for performing real-time distributed reactive power support that achieves the optimality of centrally based approaches while maintaining a decentralized control architecture. Our approach does not rely on system models, communications between agents, or large deployments of additional sensors. To achieve this, we utilize a model-free control algorithm known as Extremum Seeking (ES) [7]. ES has been used in a variety applications

Daniel B. Arnold and David M. Auslander are with the Dept. of Mechanical Engineering, U.C. Berkeley. Matias Negrete-Pincetic is with the EECS Dept., U.C. Berkeley and the Electrical Engineering Department at Pontificia Universidad Catolica de Chile. Emma M. Stewart is with the Environmental Energy Technologies Division at Lawrence Berkeley National Laboratory, Duncan Callaway is with the Energy and Resources Group, U.C. Berkeley. This work was supported in part by Robert Bosch LLC through its Bosch Energy Research Network funding program and in part by the U.S. Department of Energy ARPA-E program (DE-AR0000340) and NSF CPS award no. 1239467.

TABLE I: ES Design Parameters.

a_i	amplitude of probing signal for i^{th} controller
ω_i	angular frequency of probing signal for i^{th} controller
h_i	highpass filter critical frequency for i^{th} controller
l_i	lowpass filter critical frequency for i^{th} controller
c_i	integrator gain for i^{th} controller

including: robotic motion control [8]-[9], photovoltaic MPPT [10], wind energy conversion [11], and automotive engine control [12]. The algorithm utilizes a periodic probing signal to perform real time optimization over objective functions which can be nonconvex (provided the probing signal is sufficiently exciting).

The main contribution of this work is to demonstrate that multiple four quadrant inverters, each controlled by an independent ES algorithm, can supply reactive power to minimize feeder head real power consumption without any explicit knowledge of the feeder itself. The only sensing information required by the ES controller is knowledge of feeder head real power, which can be relatively easily broadcast from the substation.

This paper is outlined as follows. Section II introduces the ES control algorithm and the objective function for distributed reactive power support. In Section III, we explore the performance of ES-controlled inverters for a 13 node distribution system and compare results against an existing centralized approach based on a convex relaxation of the problem. We then provide concluding remarks in Section IV.

II. Analysis

A. ES Algorithm

Fig. 1 outlines the ES algorithm used to control a single inverter. In our framework, multiple inverters are controlled by independent control loops. The subscript i indexes the control loop and allows for different loops to be heterogeneously parameterized. As is shown in the figure, the algorithm injects a periodic perturbation signal into the objective function. The output of the objective block, f_i, is passed through a washout filter to eliminate low frequency content. This signal is then demodulated with a sinusoid of the same frequency as the perturbation, passed through a lowpass filter, and then integrated with gain $-c$. The resulting signal, $\hat{u}_i$ can be thought of as an estimate of the gradient of the objective function. Low and highpass filters are not necessary for convergence, but serve to smooth $\hat{u}_i$. This signal is then added to the excitation signal and fed back into the plant, u_i. Control design parameters of a single loop are summarized in Table I.

The authors of [13] provide sufficient conditions for asymptotic stability of the feedback interconnection of Fig. 1 and show that the ES feedback controller mimics a gradient-based descent algorithm in driving the control variable u_i to the optimum of the objective. In addition, [7] establishes that

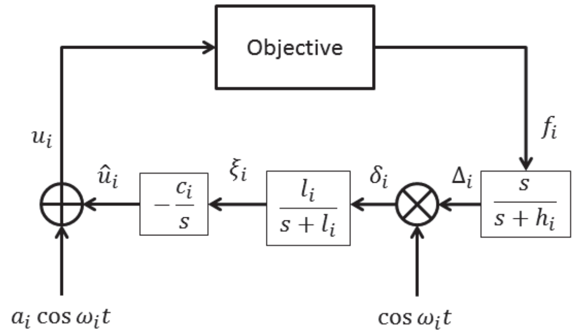

Fig. 1: Block diagram for *Extremum Seeking* control algorithm.

multiple ES control loops operating on the same objective function do not "fight" each other, provided their probing frequencies are unique. The problem considered herein deals with the injection of reactive power into a single distribution circuit in the absence of knowledge of feeder load dynamics. In practice, this information is almost assured to be unavailable. High and lowpass filters are tuned to reject dynamics in load data away from individual probing frequencies.

It is easily verified that the stability conditions of [13] are satisfied by an objective function that is convex with respect to the control variables u_i. Therefore, we will focus on establishing that this relationship holds for feeder head real power with respect to multiple injections of reactive power anywhere on a feeder.

B. Objective Function Construction

Let $T = (H, E)$ denote rooted tree graph representing a balanced radial distribution feeder, where H is the set of nodes of the feeder and E is the set of line segments. Nodes are indexed by $i = 0, 1, \ldots, m$, where m is the order (number of nodes) of the graph T. In this formulation, node 0 denotes the feeder head (or substation) and is the root of T. We treat the feeder head as an infinite bus, decoupling interactions in the downstream distribution system from the rest of the grid. This approximation is common in distribution system control design (see [14] for an example). Because of this, we assume that the voltage at node 0 is fixed and independent of control actions in the feeder.

For all $i \in H$ let y_i denote the *squared* magnitude of the node voltage. For adjacent nodes i and j, the power/voltage relationship is captured by the *DistFlow* [15] equations:

$$P_i = p_i + \sum_{j:(i,j)\in E} P_j + \frac{r_{ij}}{y_j}\left(P_j^2 + Q_j^2\right) \tag{1}$$

$$Q_i = q_i + u_i^q + \sum_{j:(i,j)\in E} Q_j + \frac{x_{ij}}{y_j}\left(P_j^2 + Q_j^2\right) \tag{2}$$

$$y_i = y_j + 2r_{ij}P_j + 2x_{ij}Q_j + \frac{r_{ij}^2 + x_{ij}^2}{y_j}\left(P_j^2 + Q_j^2\right)$$
$$\forall j : (i,j) \in E. \tag{3}$$

In the system of (1) - (3), node i real and reactive power demands are denoted by p_i and q_i, respectively. In our convention, positive demand denotes power consumption and negative demand is power injected, or supplied, to the grid. In this formulation, P_j and Q_j represent the real and reactive power that flows into node j from node i, over line segment (i,j). The terms r_{ij} and x_{ij} are rectangular components of edge (i,j) electrical impedance and are assumed to be positive. The quantity u_i^q represents reactive power that can either be sourced or consumed by a smart grid component.

The problem we are interested in solving is an Optimal Power Flow (OPF) problem where the objective is to minimize real power supplied by the distribution substation to the rest of the feeder. We define the problem as

$$\begin{aligned} J = \min P_0 & \\ \text{subject to:} \quad & (1) - (3) \\ \text{over:} \quad & P_i, Q_i, y_i, u_i^q, \quad i \in H \end{aligned} \tag{4}$$

where we are currently ignoring constraints on the voltage magnitudes and line power flow constraints. The effect of our control algorithm on these constraints is considered in detail in separate works. The only constraints in this simplified OPF are the equality constraints that govern the physics of the real/reactive power and voltage relationship between adjacent nodes in the feeder. These equality constraints are nonlinear and, in general, nonconvex. The OPF problem can be transformed into a convex program through the use of convex relaxations, and a substantial body of work exists dealing with these issues [4], [6], [5]. However, such approaches are not well suited to the problem considered here, as the ES control algorithm is feedback-based and does not allow for the relaxation of the physics of the system.

The problem of (4) is alternatively represented through successive substitutions of (1) - (3), into P_0. This process eliminates all variables P_i, Q_i, and y_i. The new objective function, f, can be thought of as a mapping from $\Re^m \to \Re$ and is completely unconstrained:

$$J = \min_{u_i^q, i \in H} P_0 = f(u_1^q, \ldots, u_m^q). \tag{5}$$

If the objective function of (5) is convex, we will have satisfied sufficiency conditions guaranteeing the stability of the ES control algorithm.

C. Convexity Analysis

Here we show that the objective of (5) is convex with respect to injected reactive powers, u_i^q. To begin, consider a distribution feeder represented by T. Let m represent the order (i.e. number of nodes) of T and $\bar{u}$ is the vector of all controllers (u_i^q) at nodes in H, where $\bar{u} = [u_1^q, \ldots, u_m^q]^T \in \Re^{m \times 1}$. Without loss of generality, we assume a controller, u_i^q, exists at every node in H. Nodes without the ability to inject/sink reactive power can be accommodated by setting $u_i^q = 0$. For a node $i \in H$, denote the Hessians of P_i and Q_i with respect to $\bar{u}$ as $\nabla_{\bar{u}}^2 P_i \in \Re^{m \times m}$, $\nabla_{\bar{u}}^2 Q_i \in \Re^{m \times m}$ respectively. In addition, denote the Hessian of y_i with respect to $\bar{u}$ as $\nabla_{\bar{u}}^2 y_i \in \Re^{m \times m}$. Finally, denote the gradients of P_i, Q_i, and y_i with respect to $\bar{u}$ as $\nabla_{\bar{u}} P_i \in \Re^{1 \times m}$, $\nabla_{\bar{u}} Q_i \in \Re^{1 \times m}$, and $\nabla_{\bar{u}} y_i \in \Re^{1 \times m}$ respectively. The following theorem outlines the regions under which the Hessians $\nabla_{\bar{u}}^2 P_i$ and $\nabla_{\bar{u}}^2 Q_i$ are positive semidefinite and $\nabla_{\bar{u}}^2 y_i$ are negative semidefinite.

Theorem 1: Suppose that for all $i,j \in H$, $(i,j) \in E$, where i is electrically upstream (closer to the distribution substation) friom j, the variables P_j, Q_j, and y_j satisfy the following:

D1: $1 + 2\frac{r_{ij}}{y_j} P_j \geq 0$

D2: $1 + 2\frac{x_{ij}}{y_j} Q_j \geq 0$

D3: $1 - \left(\frac{P_j^2 + Q_j^2}{y_j^2}\right)\left(r_{ij}^2 + x_{ij}^2\right) \geq 0$

D4: $2r_{ij} + 2\frac{r_{ij}^2 + x_{ij}^2}{y_j} P_j \geq 0$

D5: $2x_{ij} + 2\frac{r_{ij}^2 + x_{ij}^2}{y_j} Q_j \geq 0$

D6: $\left(1 + 2r_{ij}\frac{P_j}{y_j}\right)\frac{1}{\alpha_j} + 2r_{ij}\frac{Q_j}{y_j} \geq 0$

D7: $\left(1 + 2x_{ij}\frac{Q_j}{y_j}\right)\frac{1}{\beta_j} + 2x_{ij}\frac{P_j}{y_j} \geq 0$

D8: $\left(\frac{\alpha_i}{\alpha_j} - 1\right) + \left(\frac{2P_j}{\alpha_j y_j} + \frac{2Q_j}{y_j}\right)(\alpha_i r_{ij} - x_{ij}) \geq 0$

D9: $\left(\frac{\beta_i}{\beta_j} - 1\right) + \left(\frac{2Q_j}{\beta_j y_j} + \frac{2P_j}{y_j}\right)(\beta_i x_{ij} - r_{ij}) \geq 0$

Where α_i and β_i are defined according to:

$$\alpha_i = \max_{j \in H, (i,j) \in E} \left[\max\left(\frac{x_{ij}}{r_{ij}}, 2\alpha_j - \frac{x_{ij}}{r_{ij}}\right)\right] \tag{6}$$

$$\beta_i = \max_{j \in H, (i,j) \in E} \left[\max\left(\frac{r_{ij}}{x_{ij}}, 2\beta_j - \frac{r_{ij}}{x_{ij}}\right)\right]. \tag{7}$$

Then the following results hold $\forall i \in H$, where v is any nonzero vector:

R1: $v^T \nabla_{\bar{u}}^2 P_i v \geq 0$

R2: $v^T \nabla_{\bar{u}}^2 Q_i v \geq 0$

R3: $v^T \nabla_{\bar{u}}^2 y_i v \leq 0$

The proof is omitted for space constraints, but is based on induction from the leaves of the distribution feeder. The constraints **D1** - **D9** limit the allowable amount of reverse power flowing in each line segment of the circuit and are dependent on the downstream feeder topology and impedance ratios. If the amount of reverse flow is not too large, then P_i and Q_i are convex and y_i are concave for all $i \in H$. Constraints **D1** - **D9** typically allow for reverse real and reactive power flows on the order of several times the per unit rating of the feeder and are, therefore, virtually always met during standard feeder operations. In other works, we throughly explore the convexity proof as well as reverse flow constraints for different feeder topologies.

III. Simulation Results

In order to test the optimality of the ES control algorithm, simulations of smart inverters interacting with a 13 node balanced distribution feeder model were conducted. The feeder model can be found in [16] and is depicted in Fig. 2. In these tests, the smart inverters were located at nodes 3, 8, and 9 and loads were located at nodes 1, 5, 7, 8, 11, and 12.

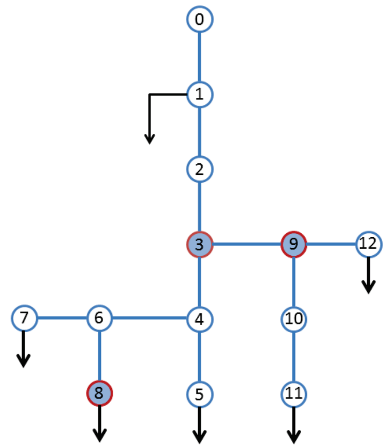

Fig. 2: Feeder model used in simulations [16]. Nodes in red indicate where smart inverters controlled by ES are located.

In order to confirm that feeder head real power is minimized when reactive power injection is controlled by the ES algorithm, an experiment was performed using a single inverter located at node 3 and constant feeder loading. These results were compared to a baseline case that was known *a priori* to produce optimal results [4].

The results of the constant load test can be found in Fig. 3, that depicts feeder head reactive power in three cases: 1) a baseline case, 2) the simulation results of the ES controller, and 3) the result obtained from use of the techniques in [4] (i.e., the *optimal* results). This plot shows the reactive power that is supplied to the rest of the feeder by the distribution substation. In this experiment, feeder loads were fixed at 0.5 VA p.u. with a power factor of 0.9. For a one hour test with timesteps of 0.1 seconds, Fig. 3 plots only every thousandth data point. The figure shows the control signal oscillating slightly around the optimal value and this behavior is expected due to the dither of the ES controller.

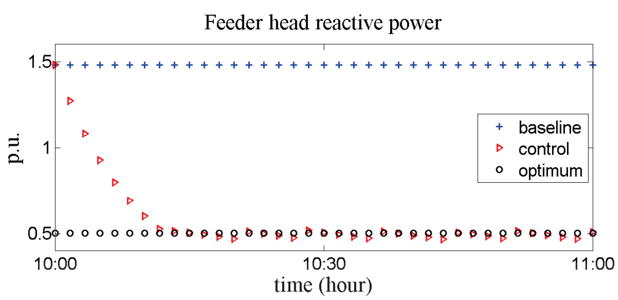

Fig. 3: Substation reactive power during constant load test.

In a second experiment, the response of multiple ES controllers in the presence of time-varying loads was tested. The simulation was driven by publicly available 30 minute demand information (kW) from the Pacific Gas and Electric Company (a large California utility) [17]. This data was interpolated over the duration of a 3 hour experiment with

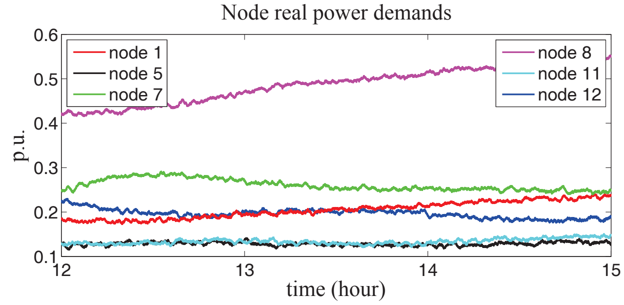

Fig. 4: Real power demands on the 13 node feeder.

TABLE II: Simulation Parameters

Parameter	Node 3	Node 8	Node 9
f (Hz)	$\frac{\sqrt{2}}{100}$	$\frac{\sqrt{3}}{100}$	$\frac{\sqrt{5}}{100}$
h $(\frac{rad}{s})$	2.5×10^{-4}	2.5×10^{-4}	2.5×10^{-4}
l $(\frac{rad}{s})$	1×10^{-4}	1×10^{-4}	1×10^{-4}
c	-2	-2	-2
a (p.u.)	0.0025	0.0025	0.0025
UB (p.u.)	0.1	0.125	0.15
LB (p.u)	-0.1	-0.125	-0.15

timesteps of 0.1 seconds. A constant power factor of 0.9 was used to create reactive power demands and filtered zero mean Gaussian noise of variance 0.001 was added to all real and reactive load data. Filtered noise data introduced autocorrelation into the demand profiles that is expected to exist in more granular data. The individual real power demand profiles are shown in Fig. 4. Future works will investigate the effectiveness of ES control using higher resolution (1 minute) demand information.

During the experiment, all feeder line segments had an impedance of $Z = 0.3 + j0.6\ \Omega$ and base values for voltage and power were 7200 V and 1 MVA, respectively. The voltage at the feeder head was fixed at 1 p.u. with 0 phase angle. Simulation parameters for the three ES controllers are given in Table II. Here, UB and LB refer to the upper and lower bounds on allowable reactive power injection/consumption.

Simulation results of the second experiment are shown in Figs. 5 - 9, which show the ES controlled inverters steadily injecting reactive power into the system until all become saturated. This action results in an improvement in the system voltages (illustrated at node 4, in Fig. 6) as well as reductions in reactive and real power supplied to the circuit by the distribution substation (see Figs. 7 and 8, respectively). Fig. 9 shows a closeup of inverter reactive power output after saturation. Note that the amplitude of the probing signals of the ES controllers are on the order of 0.25% of the rated power of the feeder.

IV. Concluding Remarks

This work shows that optimal real power minimization using distributed reactive power resources can be accomplished in real-time, *without* knowledge of any system models or

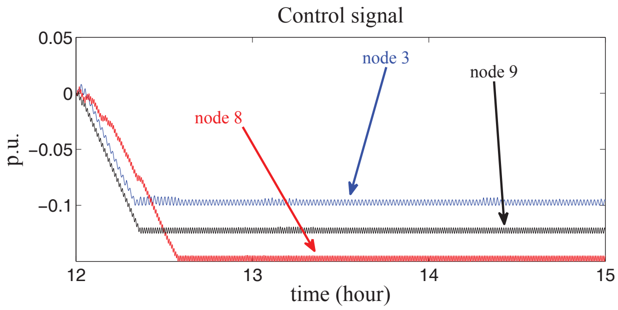

Fig. 5: Reactive power output of controllable inverters.

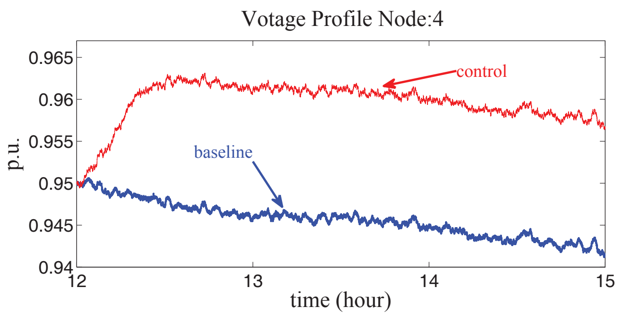

Fig. 6: Node 4 voltage profile during the simulation.

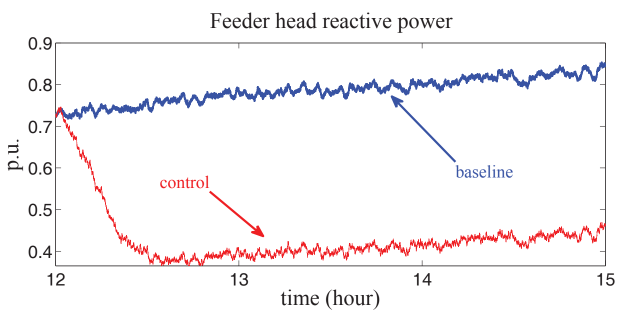

Fig. 7: Feeder head reactive power

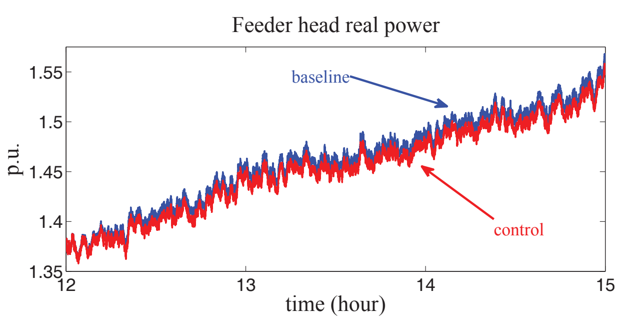

Fig. 8: Feeder head real power

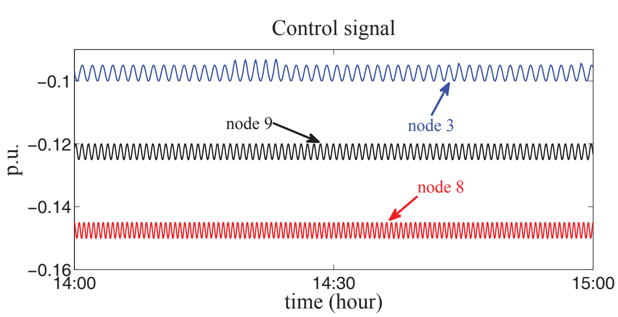

Fig. 9: Closeup of control residuals.

communication between decision-makers, and based solely on a single feedback measurement from the substation. Having demonstrated the efficacy of the use of ES to control inverters in this manner, the door is now open to consider non-model based techniques as practical and more easily-implementable solutions than their model-based counterparts. Upcoming works will explore the effect of ES-controlled inverters for voltage regulation, and will investigate control algorithm performance using 1 minute real power demand data.

REFERENCES

[1] E. M. Stewart, S. V. MacPherson, D. Nakafuji, and T. Aukai, "Analysis of high-penetration levels of photovoltaics into the distribution grid on oahu, hawaii, detailed analysis of heco feeder wf1," NREL subcontract report NREL/SR-5500-54494, Tech. Rep.

[2] K. Turitsyn, P. Sulc, S. Backhaus, and M. Chertkov, "Options for control of reactive power by distributed photovoltaic generators," *Proceedings of the IEEE*, vol. 99, no. 6, pp. 1063–1073, 2011.

[3] J. Smith, W. Sunderman, R. Dugan, and B. Seal, "Smart inverter volt/var control functions for high penetration of pv on distribution systems," in *IEEE Power Systems Conference and Exposition (PSCE)*. IEEE, 2011, pp. 1–6.

[4] M. Farivar, C. R. Clarke, S. H. Low, and K. M. Chandy, "Inverter var control for distribution systems with renewables," in *IEEE International Conference on Smart Grid Communications (SmartGridComm)*. IEEE, 2011, pp. 457–462.

[5] A. Lam, B. Zhang, A. Dominguez-Garcia, and D. Tse, "Optimal distributed voltage regulation in power distribution networks," *arXiv preprint arXiv:1204.5226*, 2012.

[6] E. Dall'Anese, G. B. Giannakis, and B. F. Wollenberg, "Optimization of unbalanced power distribution networks via semidefinite relaxation," in *North American Power Symposium (NAPS), 2012*. IEEE, 2012, pp. 1–6.

[7] K. B. Ariyur and M. Krstic, *Real-time optimization by extremum-seeking control*. John Wiley & Sons, 2003.

[8] C. Zhang, D. Arnold, N. Ghods, A. Siranosian, and M. Krstic, "Source seeking with non-holonomic unicycle without position measurement and with tuning of forward velocity," *Systems & Control Letters*, vol. 56, no. 3, pp. 245–252, 2007.

[9] D. B. Arnold, "Control of a non-holonomic unicycle via extremum seeking," Master's thesis, University of California, San Diego, 2006.

[10] A. Ghaffari, M. Krstic, and S. Seshagiri, "Power optimization for photovoltaic micro-converters using multivariable newton-based extremum-seeking," in *IEEE 51st Annual Conference on Decision and Control (CDC)*. IEEE, 2012, pp. 2421–2426.

[11] ——, "Power optimization and control in wind energy conversion systems using extremum seeking," in *American Control Conference (ACC)*. IEEE, 2013, pp. 2241–2246.

[12] N. J. Killingsworth, S. M. Aceves, D. L. Flowers, F. Espinosa-Loza, and M. Krstic, "Hcci engine combustion-timing control: Optimizing gains and fuel consumption via extremum seeking," *IEEE Transactions on Control Systems Technology*, vol. 17, no. 6, pp. 1350–1361, 2009.

[13] M. Krstić and H.-H. Wang, "Stability of extremum seeking feedback for general nonlinear dynamic systems," *Automatica*, vol. 36, no. 4, pp. 595–601, 2000.

[14] B. A. Robbins, C. N. Hadjicostis, and Domínguez-García, "A two-state distributed architecture for voltage control in power distribution systems," *IEEE Transactions on Power Systems*, vol. 28, no. 2, pp. 1470–1482, 2012.

[15] M. E. Baran and F. F. Wu, "Optimal sizing of capacitors placed on a radial distribution system," *IEEE Transactions on Power Delivery*, vol. 4, no. 1, pp. 735–743, 1989.

[16] W. H. Kersting, *Distribution system modeling and analysis*. CRC press, 2012.

[17] "PG&E Direct Access Customer Class Load Profile," http://www.pge.com/nots/rates/006f1c4_class_load_prof.shtml, [Online; accessed July-2014].